ESANN'1996 proceedings - European Symposium on Artificial Neural Networks
Bruges (Belgium), 24-25-26 April 1996, D-Facto public., ISBN 2-9600049-6-5, pp. 113-147

Biologically inspired eye movements for the visually guided navigation of mobile robots

Fabrizio MURA, Nicolas MARTIN, Nicolas FRANCESCHINI

CNRS/L.N.B. 3 Neurocybernetics Study Group
31, Chemin Joseph Aiguier
13009 Marseille - France
Phone: (33) 91 16 41 29; Fax: (33) 91 22 08 75
E-mail: mura (or) martin (or) enfranceschini@irlnb.cnrs-mrs.fr

Abstract.

Among the growing number of 'bionic' approaches which have been developped recently to address the problem of visually guided navigation, two biologically inspired eye movement strategies are described here which were designed to enhance the ability of a terrestrial mobile robot to perceive *visual motion* . The ideas which led to these developments were largely based on the observation of specific retinal movements occurring in the fly's compound eye [13], [8], [10]. The philosophy underlying this work is closely linked to the concept of *active perception* [2], [24], [1], [25]: a mobile agent is likely to ease off a considerable amount of the computational burden involved in visual processing by generating some specific eye movements during its own motion. Two different types of eye movements are proposed here: *corrective vergence* and *scanning* vergence. Our findings show that both enhance the ability of a mobile agent to detect the contrasting obstacles in a stationary environment. With the help of our robotic demonstrators, these simulations should also contribute to clarifying the functional role of some enigmatic eye movements which have been found to occur in biological systems.

1. Introduction

In the framework of our studies on the perception of visual motion, we present here some of the laboratory's recent research on active eye movements as a means of assisting vision of mobile robots. Our ideas for introducing eye movements into a robotic device were mainly inspired by biological findings on arthropods' eye movements [13], [6], [8], [16], [10] and our goal here was to investigate two possible strategies for eye movements in the context of motion perception. We wanted to establish whether the controlled movement of a sensor designed to detect motion might help a sighted mobile robot navigate. The function of these eye movements is closely linked to the detection of moving visual contrasts: the characteristics of the eye movements (such as the type of movement, its amplitude and frequency) are not necessarily dependent on the structure of the eye or on the motion pattern of the platform on which it is mounted. Interestingly, implementing 'mobile eyes' onboard a mobile platform requires no major structural changes in the motion detector's electrical circuits, since endowing the eye with movement does not affect the basic functional principles involved in the perception of *visual motion*.

ESANN'1996 proceedings - European Symposium on Artificial Neural Networks
Bruges (Belgium), 24-25-26 April 1996, D-Facto public., ISBN 2-9600049-6-5, pp. 113-147

This research is the logical outcome of the previous robotic experiments performed at our laboratory [23], [9]. The validity of the theoretical principles on which the eye movements were based has been previously demonstrated via computer simulations [17], [20], and it is proposed here to confirm their feasibility in a complete visuomotor loop. As shown in section §2.1, the rationale behind the implementation of active eye movements was based on the analysis of the visual constraints involved in visual motion detection [23].

2. What is visual motion?

The large body of biological data available on visually guided behaviour in insects and vertebrates has given birth to some novel approaches, ideas and concepts in artificial intelligence and artificial vision [3], [23], [28], [4], [25]. From the theoretical point of view, the principle of *motion parallax* [26], [7] is a milestone in the field of visual perception. According to this principle, any moving observer performing a pure translation in a static environment will perceive a coherent *optic flow field* [14], [22], [15], as given by the matrix of the local angular velocities of the light-contrasted images of the obstacles encountered. Thus, in the case of a 2D environment comprising a given contrast point M (Fig.1) oriented at φ with respect to the observer's line of travel, and located at distance D from the eye O of the observer, the apparent angular velocity of M induced by the observer's own movement is [11], [27]:

$$\Omega = V/D \cdot \sin(\varphi) \qquad \text{equation (1)}$$

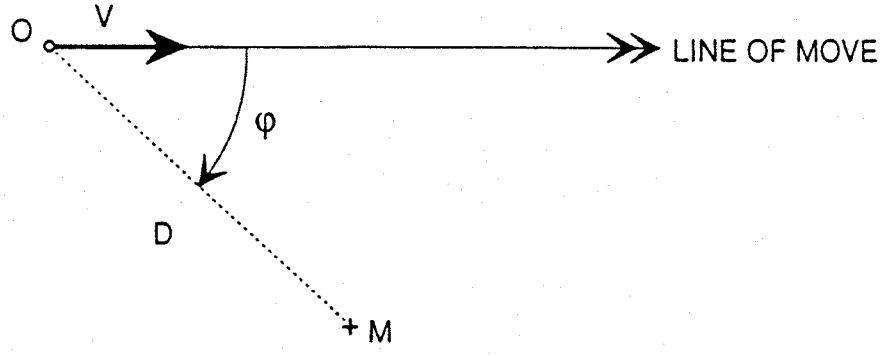

Fig. 1. Principle of motion parallax relating the angular velocity Ω of a feature point M to its azimuthal orientation φ with regard to the observer's line of travel, to its distance D and to the observer's speed V

Equation (1) has already been adapted to the case of a 2D horizontal plane, where a single panoramic compound eye with 118 visual directions enabled a small wheeled platform to reach a visual target at a relatively high speed (0.5m/s), while avoiding oncoming obstacles [23]. Their prototype features a visuomotor loop entirely based on a chain of analog circuits which process the visual signals in a purely

ESANN'1996 proceedings - European Symposium on Artificial Neural Networks
Bruges (Belgium), 24-25-26 April 1996, D-Facto public., ISBN 2-9600049-6-5, pp. 113-147

parallel manner, starting from the photodiode amplifiers and continuing down to the control loop of the steering motor [9]. Upstream from the navigation algorithm, the visual system delivers an analog value of the local angular velocity Ω in the direction of every visual axis, thanks to a basic circuit called the 'Local Motion Detector' (LMD). Every LMD in the compound eye is able to measure the relative movement of a light-contrasted obstacle passing across its two adjacent visual axes. Let us note that there exist fundamental differences between the measuring technique of the LMD and the majority of the existing optic flow techniques based on the analysis of successive 'frames' of CCD images:

_ the LMD is a repeat circuit driven by two adjacent ommatidia, each of which is provided with its own edge contrast detector circuit

_ In the LMD, the temporal acquisition of the movement is *continuous*, since any variations in the light intensity are detected during the robot's own motion, thanks to a hardwired analog circuit. The contrast detection performances therefore depend only on the bandwidth of the analog band-pass filters.

2.1 What are the constraints involved in reflexive visuomotor navigation?

Working with a purely reflexive control algorithm means that the robot's state is likely to depend on the latest measurements picked up instantaneously by the sensor: the robot neither relies on any memory of past data, nor does it need to use a global representation of the environment in order to steer its way. In theory, the acquisition of the angular velocities is a purely *asynchronous* process, since the visual inputs depend on the state of the robot within the surroundings, namely its position, orientation and speed. In order to obtain an acquisition strategy which fits the manoeuvrability of the platform, a finite time cycle with a constant duration ΔT, termed the *visual acquisition cycle* was introduced [23], [17], [19]. This means that the angular velocities are measured and buffered during ΔT so that the robot reacts at the end of each visual acquisition cycle, on the basis of the data collected during this cycle. This operating mode, termed the 'asynchronously synchronized' acquisition mode, was used successfully to guide the steps of the first prototype [23,9] with a constant value of ΔT of 0.2s.

The drawbacks of this strategy are twofold. First of all, during ΔT, the robot remains in an 'open loop' in the sense that it cannot undergo a change of state before the end of ΔT. Secondly, by maintaining a constant value of ΔT during the whole trajectory of the robot, we impose a limitation on the range of vision R_V of the visual sensor. Indeed, a constant value of ΔT means that a given LMD will be able to measure only the angular velocities greater than a minimum value Ω_{min} such that:

$$\Omega_{min} = \Delta\varphi/\Delta t \qquad (2)$$

where $\Delta\varphi$ is the interommatidial angle between the two adjacent visual axes of a given LMD. The constraint of equation (2) can be rewritten as two separate constraints affecting the *maximum range of vision* (R_V) of the LMD, as a function of the orientation of its visual axes and the robot's speed of translation. In fact, by combining equation (1) and equation (2), we obtain the following expressions for these split constraints:

ESANN'1996 proceedings - European Symposium on Artificial Neural Networks
Bruges (Belgium), 24-25-26 April 1996, D-Facto public., ISBN 2-9600049-6-5, pp. 113-147

$R_V = V/\Omega_{min} \cdot \sin(\varphi)$ thus: $R_V \sim V$ for a given value of φ (3)

$R_V \sim \sin(\varphi)$ for a given value of V (4)

Equation (3) gives the *kinematic constraint* involved in visual motion. It states that the maximum range of vision R_V of a given LMD is proportional to the robot's speed of translation: the faster the robot travels, the larger the range of vision will become. Equation (4) gives the *geometric constraint* involved in visual motion: at a given speed the robots's range of vision is proportional to the sine of the orientation with respect to the heading direction. For example, with a uniform angular distribution of visual axes (i.e., if $\Delta\varphi$ is independent of φ), R_V will be smallest when $\varphi \approx 0°$ and largest when $\varphi = 90°$. Hence, solving the problem of the visual control of the trajectory of the terrestrial robot can be said to meet the two aforementioned constraints imposed by the visual acquisition loop.

The first solution was proposed by [23], who dealt with the geometrical constraint by designing a specific angular configuration of the compound eye, as shown in figure 2a. The panoramic compound eye, composed of 102 visual directions arranged according to a sine-law gradient, was assisted by two secondary off-centered eyes, each of which had only 8 visual axes and sampled half the frontalmost visual field. The resulting configuration yielded a range of vision which was quasi-circular in shape (there was a narrow blind zone in the posterior part). The kinematic constraint was met by defining a specific pattern of motion for the robot. After being launched at a constant translatory speed, the robot reacted using a near-minimum collision avoidance strategy. Whenever it was forced by an obstacle to change course, the obstacle avoidance algorithm computed the requisite amplitude of the subsequent steering lock. At the end of the current visual acquisition cycle, the robot came to a halt, performed a corrective pure rotation and resumed its translatory movement for the next acquisition cycle. It is important to note that the visual loop had to be inhibited during the corrective steering manoeuvres because during any rotation the perceived angular velocities of surrounding objects does not depend on their distance [22], [15], [19], and therefore could not possibly inform the robot about the proximity of the obstacles. Furthermore, in order to detect any oncoming obstacles, a 'safety circle' centered on the platform was introduced , the radius of which was smaller than the eye's range of vision.

3. Meeting the constraints via controlled 'vergence' eye movements

The first mobile robot prototype successfully avoided collisions by travelling at a constant translatory speed, thereby maintaining a constant range of vision during motion [9]. Its construction was followed by another project where the objective was to evaluate a robust navigation algorithm which could adapt the forward speed to the density of the looming obstacles [17], [18]. This robot has the same circular body, the same kinematics and a visual sensor with the same angular configuration as the previous one (see figure 2a). The platform is allowed, however, to move at variable translatory speeds. In order to navigate safely, the robot adjusts its speed so as to maintain a *permanent visual contact* with the obstacles while avoiding them: in this way, whenever the robot approaches an obstacle at a speed V higher than the

ESANN'1996 proceedings - European Symposium on Artificial Neural Networks
Bruges (Belgium), 24-25-26 April 1996, D-Facto public., ISBN 2-9600049-6-5, pp. 113-147

minimum value V_{min}, it evaluates the requisite deceleration on the basis of the angular velocity and orientation of the detected obstacle. The deceleration is calculated in such a way that at the next acquisition cycle, the range of vision R_V (equ. (3)) is reduced so as to guarantee that the same obstacle is being detected with a given value of angular velocity. However, when the translatory speed reaches a value defined as a threshold, and the eye still detects an obstacle on its path, the robot stops at the end of the acquisition step and changes course by turning around its centre of gravity. The velocity threshold is defined such that the robot still can make one translation towards the obstacle without touching it. Again, the corrective steering lock is computed on the basis of a near-minimum obstacle avoidance strategy.

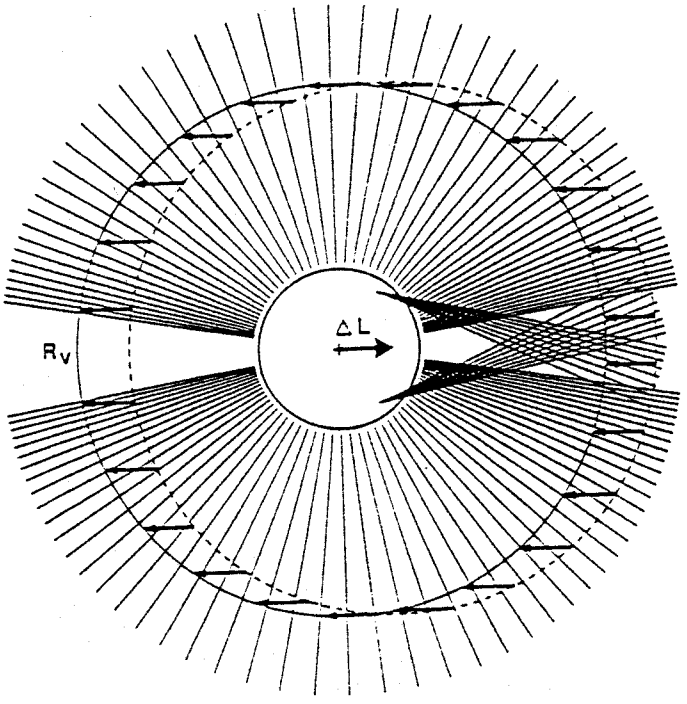

Fig 2a. Overview of the complete, 2D angular configuration of the LMD-eye initially designed [23] and constructed [9]. It comprises a quasi-panoramic compound eye with 102 ommatidia and hence 102 visual directions (51 for each hemifield) radiating from a common centre, which is also the centre of the (circular) mobile platform. They sample the plane according to a 'sine-law gradient', thus yielding a constant range of vision in all directions. In addition, two off-centered LMD eyes, each having only 8 visual axes, are placed symmetrically with respect to the midline of the eye, which is always oriented along the robot's line of travel (from [23], [9]).

ESANN'1996 proceedings - European Symposium on Artificial Neural Networks
Bruges (Belgium), 24-25-26 April 1996, D-Facto public., ISBN 2-9600049-6-5, pp. 113-147

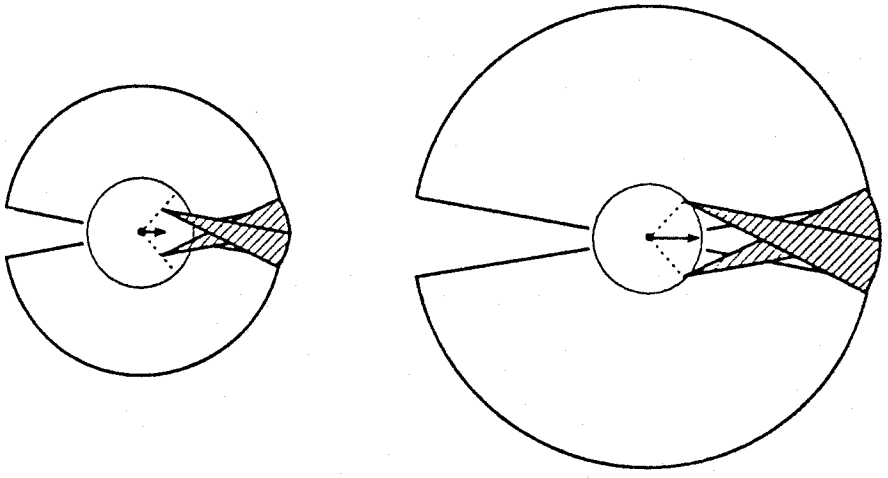

Fig. 2b. In order to maintain a circle of vision at the various translatory speeds, the optical centres of the two off-centered eyes are moved simultaneously (outwards in the drawing on the right side, corresponding to an increase in the speed of the robot) along symmetrical lines (dotted lines). The amplitude of these corrective 'vergence eye movements' is proportional to the translatory speed.

Whenever the speed of translation increases, the range of vision R_V of the panoramic eye increases proportionally (equ. (3)), as so does the range of vision of the two off-centred eyes. Instead of having a perfectly circular shape, the frontal part of the visual field therefore becomes distorted. In order to compensate for this distortion, one solution is to adapt the range of vision of the off-centered eyes by changing the position of their optical centre [17], as schematized in figure 2b. During an *increase* in the translatory speed, the two optical centres simultaneously move *outwards* in a linear and symmetrical manner (they move inwards during a decrease in the translatory speed). The amplitude and the direction of these unusual, outward/inward 'vergence eye movements' are computed so as to preserve the circular shape of the frontal visual space. Consequently, the robot is able to detect and avoid any obstacle which is within its circle of vision, whatever its translatory speed. This strategy was successfully simulated in a multiple task session (see figure 3), where the robot started from the point located at (150, 350) and was required to reach a target located at (1000, 350). The robot avoided the two oncoming walls, adapting its speed in a controlled manner with the help of its vergence eye movements. In figure 3 the current circle of vision was plotted at the end of each acquisition cycle. Note that, as long as no obstacles are detected ahead, the robot tends to accelerate (up to its maximum speed), and in doing so, progressively increases its range of vision. As soon as an obstacle is detected, the robot adapts its translatory speed and corrects the vergence according to the aforementioned rule which satisfies the kinematic constraint, (i.e., keeping in visual contact with the obstacles): this explains the smooth 'wall-following' behaviour observed in two parts of the trajectory.

ESANN'1996 proceedings - European Symposium on Artificial Neural Networks
Bruges (Belgium), 24-25-26 April 1996, D-Facto public., ISBN 2-9600049-6-5, pp. 113-147

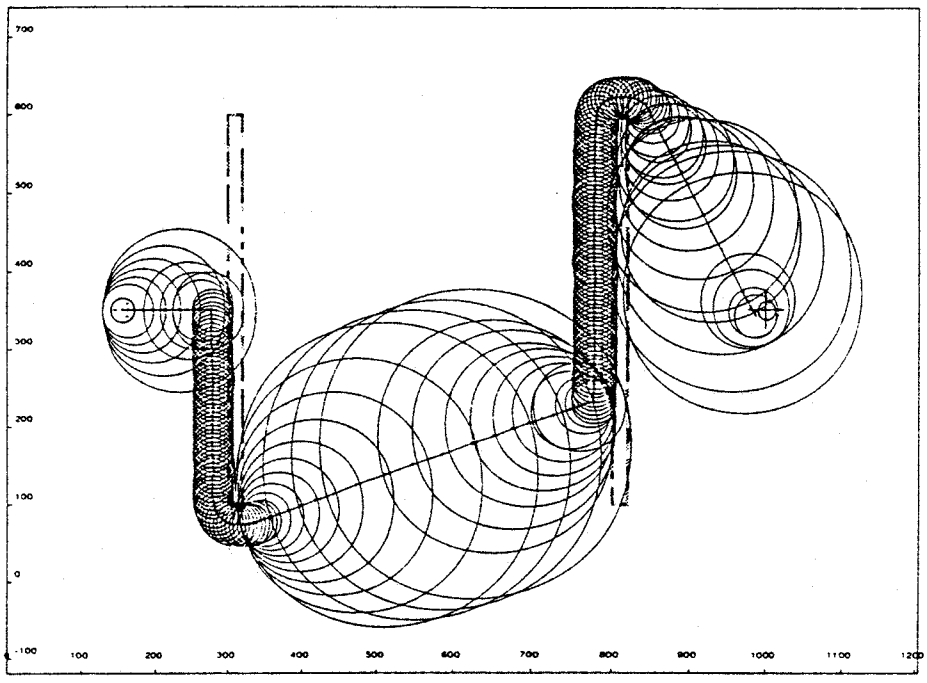

Fig. 3. Trajectory of the simulated terrestrial robot (the configuration of the eye is shown in figure 2a), with the circular range of vision plotted at the end of each visual acquisition step. After being placed at (150, 350), the robot was required to reach a target placed at (1000, 350) (the robot is able to sense only the direction of the target, not its range). It does succeed in reaching the target while adapting its translatory speed in order to avoid colliding with the obstacles (randomly textured walls) (after[17]).

To summarize, both the geometric and the kinematic constraints are met by combining a controlled vergence movement of the frontal eyes and suitably adaptating the speed of translation which ensures that the robot stays visually in contact with the obstacles during a series of visual acquisition cycles. Interestingly, this algorithm works in a purely reflexive manner so that the robot does not need any memory to be able to avoid the looming obstacles. It compensates for the absence of memory by automatically maintaining a prolonged visual contact with the environment during its own bodily motion. Much of the sensorimotor intelligence originates in the specific design of the visual sensor.

4. Meeting the constraints via 'scanning vergence' eye movements

An alternative means of tackling the problem [21] consists of having the visual axes scan smoothly in order to add a controlled *rotatory* component to the optic flow field. We know that a rotatory component is independent of the distance to the obstacles [22], [14], [15], [5]. The scanning, i.e., a controlled rotation of the visual

ESANN'1996 proceedings - European Symposium on Artificial Neural Networks
Bruges (Belgium), 24-25-26 April 1996, D-Facto public., ISBN 2-9600049-6-5, pp. 113-147

axes around the optic centre of the eye, automatically generates an appropriate rotatory angular speed. Thus, during a pure translation of the robot coupled with a rotation of the visual axes in the *anterograde direction* (i.e., with the visual axes turning from lateral to frontal), the total angular speed Ω_T of a given contrast edge measured in a robot-centred frame of reference is the linear sum of the angular speeds induced by each source of motion:

$$\Omega_T = \Omega_t + \Omega_r \qquad (5)$$

where Ω_t is the translatory angular speed and Ω_r the rotatory angular speed. In this equation, we assume that the two kinds of movement occur at constant velocities.

The added scanning movement performed during the translation of the eye will enhance the robot's ability to detect small translatory angular velocities corresponding to the slow moving image of a light-contrasted obstacle. This is particularly valuable because it enables the compound eye to detect low translatory retinal velocities in spite of its poor visual acuity: thus, the performances of the eye depend much more on the characteristics of the scanning movement than on the robot's speed of translation (the kinematic constraint vanishes progressively). In fact, the influence of the kinematic constraint and the geometric constraint depends on the angular amplitude of the smooth scanning process. We define the scanning amplitude $\Delta\xi_r$ with respect to the interommadial angle ($\Delta\varphi$) of the LMD as follows:

$$\Delta\xi_r = \alpha.\Delta\varphi \qquad (6)$$

where $\alpha \in \Re$ is termed the *scanning factor* of the LMD-eye. The most noteworthy results obtained here are:

(1) when $\alpha \geq 1$, the kinematic constraint is abolished , i. e., the range of vision R_V becomes independent of the speed of translation

(2) whenever $\alpha \geq 2$, the geometric constraint too is abolished, i.e., the range of vision R_V becomes independent of the orientation of the visual axes.

In theory, with any panoramic visual motion sensor sampling a 2D horizontal plane, the visual field of the eye covers the entire plane whenever $\alpha = 2$. This property is all the more interesting, since it does not require a specific angular sampling strategy. In order to illustrate this concept, we have drawn the visual field of the simplistic 2D panoramic sensor shown in figure 4a. This eye is omnidirectional in the plane and samples the environment uniformly with only 36 visual directions ($\Delta\varphi$ = 10°). When this eye performs an elementary translation to the right, its visual field during motion is represented by the area in black (see fig. 4b). This field is obtained by superimposing the detection field of every LMD wired between two adjacent visual axes. Consistent with the aforementioned geometrical constraint (equ. 4), the visual range is largest when $\varphi \sim 90°$ and smallest when $\varphi \sim 0°$ (fig. 4b). When, however, an anterograde scanning movement with a scanning factor $\alpha = 2$ is triggered during the same translation, the surface of the visual field increases dramatically, so as to cover the whole 2D plane, except for a narrow posterior region (fig. 4c).

The visual processing involved in what may now be termed the Scanning Local Motion Detector (SLMD) is not fundamentally different from that of the LMD circuit: both sensors measure an angular velocity, whatever its cause. The SLMD is able to

ESANN'1996 proceedings - European Symposium on Artificial Neural Networks
Bruges (Belgium), 24-25-26 April 1996, D-Facto public., ISBN 2-9600049-6-5, pp. 113-147

evaluate the translatory component by simply subtracting the (known) rotatory component induced by the controlled rotation of the visual axes.

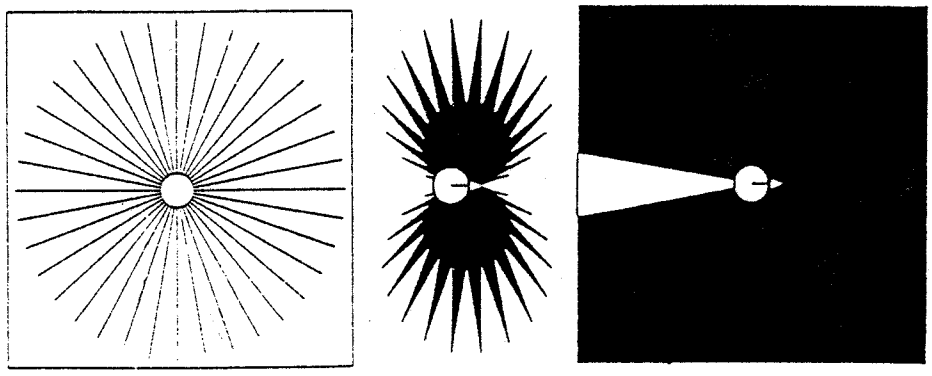

Fig. 4a (left) Simplistic panoramic eye in a 2D angular configuration. The 36 visual axes (36 pixels) are uniformly distributed (hence $\Delta\varphi = 10°$).

Fig. 4b (centre). When the eye performs an elementary translation in the left → right direction, the visual field during motion is that depicted in black: any contrast point located outside the black region will not be detected by the LMD-eye. This visual field is obtained by superimposing the field of detection of every LMD cabled behind any pair of adjacent visual axes. Note that the range of vision is largest when $\varphi \sim 90°$ and smallest when $\varphi \sim 0°$.

Fig. 4c (right). The same translatory movement coupled with an *anterograde* scanning movement of all the visual axes (scanning factor $\alpha = 2$) yields an extended visual field where the area covered includes the whole plane except for a posterior 'dead zone'.

In order to check the theoretical principles on which retinal scanning was based, we built a preliminary testbench model in the form of a scanning eye comprising a small number of visual directions (24 pixels as shown in figure 5a, [21]). Once it had been calibrated, the scanning eye was mounted on a wheeled platform and oriented in the heading direction. The angle between adjacent visual axes varied between 2.4° and 3.7°, and the total field of view of the eye was rather limited.

Thanks to a 'zig-zag' obstacle avoidance algorithm, the robot is able to move safely in a contrasted rectangular arena (see the plot of the trajectory in figure 5b). The robot is required to travel straight ahead and change course whenever an obstacle is detected in the frontal region. The evaluation of the corrective lock is based on two criteria: first of all, it must provide the robot with a safe orientation for the next translation; secondly, it must allow the robot to explore the lateral region on the side of the turn (for example, any obstacle which is detected at 30° with respect to the line

ESANN'1996 proceedings - European Symposium on Artificial Neural Networks
Bruges (Belgium), 24-25-26 April 1996, D-Facto public., ISBN 2-9600049-6-5, pp. 113-147

of travel can trigger a maximum steering lock of 90°). The plot in figure 5 was obtained during a 1 minute session, at which the robot was initially placed at the centre of the arena. The 'zig-zag' behaviour was triggered by obstacles detected in the frontal region: a previous computer simulation showed that this behaviour was vital because it provided the robot with quasi-immediate information about the presence (or absence) of obstacles in the lateral regions. In other words, the robot compensates for its inexistant lateral vision by generating a deliberately large steering angle. Consistent with other 'zig-zag' behaviours [24], [24a], the 'zig-zag' trajectory introduced here is not systematically initiated at the end of every acquisition step, but it is triggered only upon the detection of an obstacle in the frontal region, and hence is strictly dependent on visual perception. The perception of the total optic flow field by the SLMD-eye thus occurs cyclically with a period synchronized with the translatory cycles. During each visual acquisition cycle ΔT, the 12 visual axes on each side of the robot perform an anterograde scanning movement: at the end of every ΔT, the axes are rapidly shifted back to their initial orientation, so that a new scanning cycle can start.

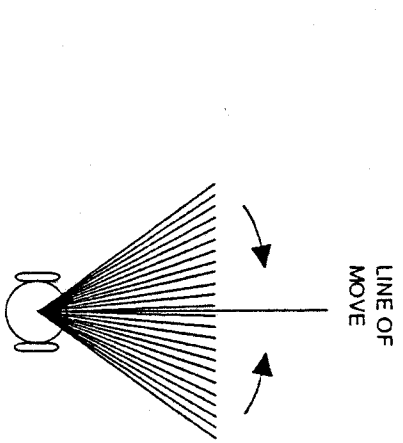

Fig 5a (left). Diagram of the terrestrial robot we constructed, with its lateral wheels and its frontal anterograde scanning (the two arrows show the scanning direction on each side of the line of travel). The monocular scanning eye comprises only 24 visual axes oriented frontally with interommatidial angles ranging from 2.4° to 3.7°. The SLMDs use the same analog circuits as the LMDs which were used in the panoramic eye of the first mobile robot developped at the laboratory [23], [9].

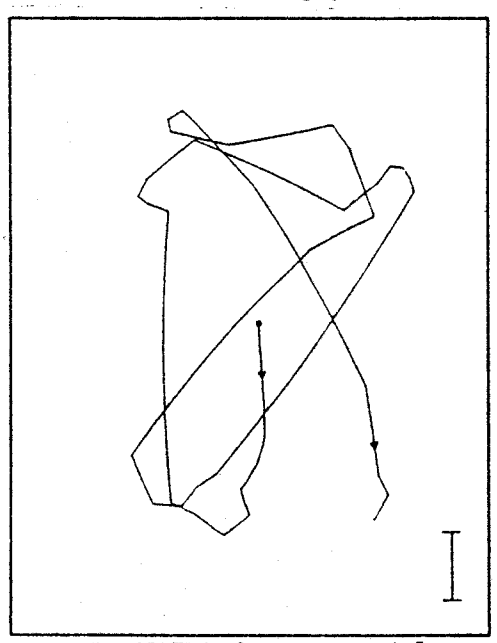

Fig 5b (right). Plot of the trajectory of the centre of the robot corresponding to a 1 minute session. The robot, moving at a constant translatory speed, is required to travel straight ahead as long as the (contrasted) walls of the rectangular arena are not detected. Whenever a wall is detected in the frontal region, the robot generates a corrective lock, using a 'zig-zag' strategy aimed at exploring the lateral region on the side of the turn, thereby compensating for its lack of lateral vision (Calibration bar = 20 cm)

ESANN'1996 proceedings - European Symposium on Artificial Neural Networks
Bruges (Belgium), 24-25-26 April 1996, D-Facto public., ISBN 2-9600049-6-5, pp. 113-147

5. Conclusion

Two different eye movement strategies are described which are liable to provide a means of satisfying the geometric and kinematic constraints associated with the perception of visual motion. The first strategy is based on the generation of corrective *vergence eye movements* in the frontal visual axes. This correction enables a mobile robot to maintain a homogeneous frontal range of vision while adapting its translatory speed, and thereby its range of vision, to the density of the objects in the surrounding environment. The second strategy consists of smoothly scanning the visual axes during the robot's own translatory motion: the visual constraints are abolished thanks to a proper choice of the scanning factor.

The strategies presented are of interest in many respects. First of all, the validity of the theoretical ideas was verified via computer simulation and the feasibility of the 'scanning vergence' movements was demonstrated by designing a hardware prototype consisting of a frontal retina mounted onboard a physical mobile robot. Secondly, the improvements do not involve making any costly changes in the visual sensor (in terms of computational power) to be able to trigger and control of the eye movements. Thirdly, the improvements do not entail any major drawbacks in the navigation algorithms, since the new robot, like its forerunner, is still able to navigate without any memory or any map of the environment. Fourthly, the theoretical background on which these results are based not only was inspired by the observation of eye movements in biological systems but suggest, in return, interesting hypotheses about the *raison d'être* of various types of eye movements observed in natural creatures.

Rather than being improved by increasing the computational power downstream, the performances of the visual sensor were enhanced right at the outset by introducing controlled eye movements. These enhanced performances do not impose any structural changes in the angular distribution of the eye's visual axes. In the case of the first solution (section 3), a circular range of vision is maintained by generating a corrective vergence movement without having to increase the visual acuity. In the case of the second solution (Section 4), the enhanced visual field and range of vision resulting from the retinal scanning procedure does not depend on the angular configuration of the eye, since the scanning amplitude can be expressed in the form of a relative scanning factor. The minimalistic design of these smart sensory systems and their low potential cost are great assets making them interesting components for incorporation into sighted mini- and micro-vehicles, for which the insect world provides plenty of models. These findings illustrate some of th e lessons which can be learned from 'humble representatives of life'. Building a smart sensory frontend can often relieve the subsequent computational burden. 'Put your money in smart sensors and not in the computer behind' could be the motto.

Acknowledgments

The authors wish to thank R. Chagneux, J. Herault and T. Netter for fruitful comments and corrections, M. Boyron and J. Roumieu for their invaluable contribution to the construction of the robot. This research was supported by the Centre National de la Recherche Scientifique (C.N.R.S. life sciences and PIR Cognisciences), the Region Provence Alpes Côte-d'Azur Corse (P.A.C.A.C.) and the

Commission of the European Communities (ESPRIT BRA SSS 6961 and HCM). F. Mura was supported by a graduate fellowship from C.N.R.S. (MREN) and N. Martin was supported by a graduate fellowship from C.N.R.S. (Engineering Science).

References

1. Y. Aloimonos: Active perception. Lawrence Erlbaum publishers, Hillsdale (USA) (1993).
2. R. Bajczy: Active perception. IEEE, 76, #8, 996-1005 (1988).
3. R. Brooks: A robust layered control system for a mobile robot. IEEE journal of Robotics and Automation,#1, 14-23 (1986).
4. D. Cliff: Computational neuroethology: a provisional manifesto. In: proc 1st Int Conf on Simulation of Adaptive Behavior SAB 90, eds Meyer & Wilson, MIT press, Cambridge (USA) 29-39 (1990).
5. D. Coombs, K. Roberts: Bee-bot: using the peripheral optic flow to avoid obstacles. In: Intelligent Robots and Computer Vision XI, SPIE 1825, 714-725 (1992).
6. A. C. Downing: Optical scanning in the lateral eyes of the copepod *Copilia*. Perception, 1, 247-261 (1972).
7. S. Exner: The physiology of the compound eyes of insects and crustaceans (English Translation 1989 by R. C. Hardie), Springer, Berlin (1893).
8. N. Franceschini, R. Chagneux, K. Kirschfeld, A. Mücke: Vergence eye movements in flies. In: proc 19th Göttingen Neurobiology Conference, eds Elsner & Penslin, 275 (1991).
9. N. Franceschini, J. M. Pichon, C. Blanes: From insect vision to robot vision. Phil Trans Roy Soc Lond B, 337, 283-294 (1992).
10. N. Franceschini, R. Chagneux: Retinal movements in freely walking flies. In: proc 22nd Göttingen Neurobiology Conference, eds Elsner & Breer, 268 (1994).
11. J. J. Gibson, P. Olum, F. Rosenblatt: Parallax and perspective during aircraft landings. Amer J Psychology, 68, 372-385 (1955).
12. T. Hamada: A neuroethological view of vision in mammals and robots. Abstract #52, Neuroethological Congress, Montreal (1992).
13. R. Hengstenberg: Eye movements in the housefly *Musca Domestica*. In: Information Processing in the Visual System of Arthropods, ed. Wehner, Springer, Berlin, 93-96 (1972).
14. B. K. P. Horn, B. G. Schunk: Determining optical flow. Artificial Intelligence, 17, 185-203 (1980).
15. J. J. Koenderink: Optic flow. Vision Research, 26, 31, 161-180 (1986).
16. M. Land: How animals scan the visual environment. In Proc IEEE Conf on Systems, Man and Cybernetics, Le Touquet (France) 144-149 (1993).
17. N. Martin, N. Franceschini: Obstacle avoidance and speed control in a mobile vehicle equipped with a compound eye. In: Proc of Intelligent Vehicles Symposium '94, ed Masaki, Paris, France, 381-386 (1994).
18. N. Martin, N. Franceschini: Environmental control of speed and steering in a sighted mobile robot: a bionic approach. In prep (1996).
19. F. Mura, N. Franceschini: Visual control of altitude and speed in a flying agent. In: Proc 3rd Int Conference on Simulation of Adaptive Behavior SAB 94, eds Cliff, Husbands, Meyer & Wilson, MIT press, Cambridge (USA) 91-100 (1994).

ESANN'1996 proceedings - European Symposium on Artificial Neural Networks
Bruges (Belgium), 24-25-26 April 1996, D-Facto public., ISBN 2-9600049-6-5, pp. 113-147

20. F. Mura, N. Franceschini: Estimation of the optic flow by motion parallax is improved by retinal scanning: I/ theoretical principles underlying retinal scanning. In prep (1996).
21. F. Mura, N. Franceschini: Estimation of the optic flow by motion parallax is improved with retinal scanning: II/ hardware implementation of an SLMD-eye for the visual guidance of a terrestrial mobile robot. In prep (1996).
22. K. Nakayama, J. M. Loomis: Optical velocity patterns, velocity sensitive neurons and space perception: a hypothesis. Perception, 3, 63-80 (1974).
23. J. M. Pichon, C. Blanes, N. Franceschini: Visual guidance of a mobile robot equipped with a network of self-motion sensors. In: Mobile Robots IV, SPIE 1195 Bellingham (USA), 44-53 (1989).
24. P. J. Sobey: Active navigation with a monocular robot. Biol Cybern, 71, 433-440 (1994).
24a.L. Steels: A case study in the behavior-oriented design of autonomous agents. In: proc 3rd int conf on Simulation of Adaptive Behavior: from animals to animats eds Cliff, Husbands, Meyer & Wilson MIT press, Cambridge (USA) 445-452 (1994).
25. T. Viéville: A few steps towards 3D active vision. Springer Series in Information Sciences, Berlin (1994).
26. H. Von Helmholtz: Optique physiologique, vol 2. Reprint from the 1962 edition, Dover publication: London (1867).
27. T. C. D. Whiteside, D. G. Samuel: Blur zone. Nature, 225, 94-95 (1970).
28. S. Wilson: The animat path to AI. In: proc 1st Int Conf on Simulation of Adaptive Behavior SAB 90, eds Meyer & Wilson, MIT press (USA) 15-21 (1990).